The Metabolic Syndrome Does Not Affect Development of Collateral Circulation in the Poststenotic Swine Kidney

Xin Zhang, [1] Seo Rin Kim, [1] Christopher M. Ferguson, [1] Behzad Ebrahimi, [1] Ahmad F. Hedayat, [1] Amir Lerman, [2] and Lilach O. Lerman [1,2]

BACKGROUND

The collateral circulation is important in maintenance of blood supply to the ischemic kidney distal to renal artery stenosis (RAS). Obesity metabolic syndrome (MetS) preserves renal blood flow (RBF) in the stenotic kidney, but whether this is related to an increase of collateral vessel growth is unknown. We hypothesized that MetS increased collateral circulation around the renal artery.

METHODS

Twenty-one domestic pigs were randomly divided into unilateral RAS fed an atherogenic (high-fat/high-fructose, MetS-RAS) or standard diet, or controls (n=7 each). RBF, glomerular filtration rate (GFR), and the peristenotic collateral circulation were assessed after 10 weeks using multidetector computed tomography (CT) and the intrarenal microcirculation by micro-CT. Vascular endothelial growth factor (VEGF) expression was studied in the renal artery wall, kidney, and perirenal fat. Renal fibrosis and stiffness were examined by trichrome and magnetic resonance elastography.

RESULTS

Compared with controls, RBF and GFR were decreased in RAS, but not in MetS-RAS. MetS-RAS formed peristenotic collaterals to the same extent as RAS pigs but induced greater intrarenal microvascular loss, fibrosis, stiffness, and inflammation. MetS-RAS also attenuated VEGF expression in the renal tissue compared with RAS, despite increased expression in the perirenal fat.

CONCLUSIONS

MetS does not interfere with collateral vessel formation in the stenotic kidney, possibly because decreased renal arterial VEGF expression offsets its upregulation in perirenal fat, arguing against a major contribution of the collateral circulation to preserve renal function in MetS-RAS. Furthermore, preserved renal function does not protect the poststenotic kidney from parenchymal injury.

Keywords: blood pressure; collaterals; hypertension; metabolic syndrome; microcirculation; renal artery stenosis; renal function.

doi:10.1093/ajh/hpy127

BACKGROUND

Renal artery stenosis (RAS) leads to gradual obstruction of the renal arterial lumen. Due to decreased blood supply and subsequent humoral and inflammatory responses, RAS may lead to hypertension and progressive kidney functional decline. In addition, RAS is linked to cardiovascular morbidity and mortality.[1] The prevalence of RAS has been growing worldwide, especially in individuals with atherosclerotic risk factors,[2,3] including obesity linked to the metabolic syndrome (MetS).

To circumvent the downstream renal ischemia, collateral circulation often ensues to convey blood supply through newly established communicating channels between the stenotic renal artery and surrounding arteries to redirect the blood to the poststenotic kidney.[4–7] The presence of collaterals is often indicative of a hemodynamically significant stenosis in both animals and humans.[8] We have previously demonstrated development of collateral circulation in RAS pigs, as well as a direct correlation of collateral growth with renal blood flow (RBF) and glomerular filtration rate (GFR),[9] which suggests a role for the collateral circulation in maintenance of renal homeostasis during decrements in renal perfusion pressure.

A large body of evidence has demonstrated that obesity affects kidney function and induces hyperfiltration, reflected by an increase of RBF and GFR. This is thought to occur mainly through vasodilatory effects of increased levels of insulin[10] and hemodynamic effects of obesity. We have also shown that RBF and GFR in RAS were preserved when superimposed by obesity MetS.[9,11] Given that obesity alone enhances intrarenal microvascular proliferation,[12,13] it may potentially augment peristenotic collateral vessel growth in RAS, which in turn would increase delivery of blood to the poststenotic kidney, thereby preserving renal function. However, it remains unknown whether the relatively preserved renal function in RAS accompanied by MetS involves augmented proliferation of collateral vessels. Therefore, this study was designed to test the hypothesis that MetS preserved renal function partly by increasing the collateral vessel growth to the distal ischemic kidney.

Correspondence: Lilach O. Lerman (lerman.lilach@mayo.edu).

Initially submitted March 2, 2018; date of first revision July 10, 2018; accepted for publication August 7, 2018; online publication August 9, 2018.

[1]Department of Medicine, Division of Nephrology and Hypertension, Mayo Clinic, Rochester, Minnesota, USA; [2]Department of Cardiology, Mayo Clinic, Rochester, Minnesota, USA.

METHODS

This project was approved by the Mayo Clinic Institutional Animal Care and Use Committee. Twenty-one domestic pigs were randomized into normal, RAS, and MetS-RAS groups ($n = 7$ each). Unilateral RAS was induced in 14 pigs by placing a local-irritant coil in 1 main renal artery, achieving subsequent hypertension within about 7 days.[14,15] MetS pigs were fed a high-fat/high-fructose diet[12] starting 6 weeks before RAS induction, and normal and RAS pigs received regular chow. Renal function and the collateral circulation were studied after 16 weeks of diet (10 weeks of RAS) using multidetector computed tomography (MDCT); the degree of stenosis was determined by angiography and *in vivo* renal stiffness (a measure of tissue fibrosis) by magnetic resonance elastography *in vivo*. Animals were then euthanized by intravenous sodium pentobarbital (100 mg/kg, Fatal Plus, Vortech Pharmaceuticals, Fort Washington, PA), and kidneys, renal arteries, and perirenal fat harvested, fresh-frozen, prepared for micro-CT (to study the intrarenal microcirculation), or preserved in formalin for staining. During MDCT studies, systemic venous blood was obtained for plasma creatinine and lipid profile, and urine collected *via* bladder puncture to determine albumin excretion. To assess insulin resistance, an intravenous glucose tolerance test was performed during MDCT in normal and MetS-RAS groups.[12] Blood samples (~3 ml each) were obtained at baseline (−5 and 0 minutes), and then animals were given an IV bolus of glucose 0.5 g/kg. Samples were obtained at 5, 10, 20, 30, 40, 50, and 60 minutes after injection to measure blood glucose and insulin levels. The homeostasis model assessment of insulin resistance index (fasting plasma glucose × fasting plasma insulin/22.5) was calculated and plotted over time to evaluate insulin sensitivity.[11]

Renal function

Single-kidney function was assessed *in vivo* using 128-slice MDCT (Somatom Definition Flash-128, Siemens Medical Solution, Forchheim, Germany).[16,17] Briefly, sequential acquisition of 140 consecutive scans was executed after a central bolus injection of iopamidol (0.5 cc/kg over 2 seconds). The first 70 scans were collected at 0.68-second intervals during respiratory suspension at end expiration, whereas the following 70 scans were acquired every 2 seconds during suspension of respiration with assisted breathing every 30 seconds. Then, MDCT images were reconstructed and displayed with the Analyze software package (Biomedical Imaging Resource, Mayo Clinic, Rochester, MN).

For data analysis, regions of interest (ROI) were selected from tomographic images from the aorta, poststenotic (or right kidney in normal pigs) renal cortex, and medulla to generate time-attenuation curves in each region and obtain measures of renal function including GFR and RBF.[18]

Collateral circulation

To collect volumetric data, the kidneys were scanned from pole to pole during infusion of iopamidol (0.5 ml/kg over 5 seconds). Reconstruction of the volume data produced 512 × 512 matrix images at a resolution of 0.39 × 0.39 mm and a 0.6-mm slice thickness with 0.3-mm overlap through the planes containing the renal artery. Collateral index was calculated by assessment of the fractional vascular volume in the immediate zone around the stenosis, as previously described.[9] Briefly, the zone encompassing visually discernible collaterals around the stenotic segment of the renal artery was manually traced (approximately 250–300 mm^2). Two ROIs were then sampled,[9] representing the collateral vessel zone surrounding the stenotic main renal artery and the contrast-filled lumen of the renal artery. In the control group, manually traced ROIs were centered on the renal artery in a comparable location. The fractional vascular area containing blood vessels around the stenosis, representing the collateral vessel fraction, was determined as the ratio between the opacity of the 2 ROIs.

Renal stiffness

As a measure of renal fibrosis, tissue stiffness was evaluated by magnetic resonance elastography (Signa TwinSpeed EXCITE 3T system, GE Healthcare, Waukeshau, WI), as described previously.[19,20] A 3D stack of images was collected using 2D, transverse, multislice, flow-compensated, spin-echo, echo-planar imaging in conjunction with motion sensitizing gradients synchronized with the 120-Hz vibrations produced by 2 passive pneumatic drivers placed on the animal's dorsal surface, proximal to the kidneys. Images were processed and analyzed using magnetic resonance elastography/Wave (MRI Research Lab, Mayo Clinic). Data were processed using phase unwrapping, curl filtration to exclude bulk motion, and a local spatial frequency estimation algorithm to determine the shear wavelength at 120 Hz. The product of shear wavelength and the vibration frequency was used to derive the shear wave speed, and the product of the tissue density (approximately 1 g/cm^3) and the square of the wave speed was used as an index of tissue stiffness. Our previous studies have shown good correlation between histological changes and stiffness in the medulla but not in cortex,[20] which is more affected by hemodynamic variables such as RBF.[19] Therefore, medullary ROIs were selected on echo-planar imaging magnitude images and verified with the aid of coregistered contrast-enhanced CT images obtained during the vascular phase of contrast agent transit.[21]

Ex vivo studies

Intrarenal microcirculation. After the harvested kidney was flushed, Microfil MV122 (an intravascular contrast agent) was perfused into the stenotic kidney under physiological pressure through a cannula ligated in the renal artery. Samples were prepared and scanned at 0.5° angular increments at 18-μm resolution, and images analyzed as described.[22,23] The spatial density of cortical microvessels (defined by diameters <500 μm) and medullary microvascular volume fraction was then calculated, as previously described.[22,24]

Expression of VEGF. To assess angiogenic signaling which is possibly involved in collateral vessel growth, expression of vascular endothelial growth factor (VEGF) was examined

in the renal artery wall and in the adjacent perirenal fat by immunohistochemistry and immunofluorescence staining, respectively. Imaging analysis was performed using a computer-aided image-analysis program (AxioVision v4.7.2.0, Carl Zeiss MicroImaging, Thornwood, NY).[17] Renal protein expression of VEGF (Santa Cruz) was also measured by western blot in homogenized kidney tissue samples. Perirenal fat gene expression of VEGF (Ss03393993) and glyceraldehyde 3-phosphate dehydrogenase (Ss03374854) was assessed on Applied Biosystems ViiA7 Real-Time PCR system using the delta-delta CT method with validated TaqMan primers from Thermo Fisher Scientific (Waltham, MA).[25]

Renal fibrosis, tubular injury, and inflammation. Renal interstitial fibrosis and glomerular score were evaluated *ex vivo* trichrome staining.[26] Tubular injury was scored in a blinded fashion in sections stained with periodic acid–Schiff, as previously described.[27] Renal inflammation was evaluated using monocyte chemoattractant protein (MCP-1, Novusbio) and tumor necrosis factor-alpha (TNF-α, Abcam) immunofluorescence staining. The number of monocyte chemoattractant protein-1 and TNF-α-expressing cells was manually counted in randomly chosen 8–10 fields/slide.[28]

Endothelial to mesenchymal transition. The endothelial to mesenchymal transition (EndoMT) was evaluated as a mechanism contribution to fibrosis and microvascular loss. Vimentin (Abcam) and CD31 (Bio-Rad) antibodies were used for immunofluorescence in renal frozen sections. The numbers of cells colocalized with vimentin and CD31 were manually quantified in randomly chosen 10–15 fields/slide.[29]

Statistical analysis

Statistical analysis was performed using JMP software package version 9.0, SAS Institute, Cary, NC. Results are shown as mean ± SEM or median (interquartile range) as appropriate. For data with normal distribution, one-way analysis of variance was applied followed by unpaired Student's *t*-test. Wilcoxon test was performed for non-normal distribution data. Pearson correlation test was performed to detect the relation between medullary stiffness and vascular volume fraction. Results were considered significant for $P < 0.05$.

RESULTS

MetS-RAS pigs had higher body weight, plasma total cholesterol, low-density lipoprotein, and triglyceride levels (Table 1). MetS-RAS developed insulin resistance, as reflected in increased baseline homeostasis model assessment of insulin resistance and in a marked increase in HOMA-IR in the glucose tolerance test compared with normal animals (Figure 1a), suggesting development of MetS. Both RAS groups developed comparable moderate degrees of stenosis (Figure 1d), and both increased mean arterial pressure, yet it was higher in MetS-RAS, consistent with pro-hypertensive effects of MetS. Plasma creatinine levels were slightly and similarly increased in both RAS groups, while urine albumin to creatinine ratio was unaltered (Table 1).

Renal hemodynamics and circulation

RBF and GFR decreased in the stenotic RAS kidney (Figure 1b,c), confirming a hemodynamically significant stenosis. However, despite a comparable obstruction of renal artery (Table 1, Figure 1d), RBF and GFR were not lower than normal in MetS-RAS (Figure 1b,c), suggesting relatively preserved renal function. Interestingly, however, both RAS and MetS-RAS similarly increased collateral index surrounding stenotic renal artery (Figure 1d,f). Within the kidney, microvascular loss was found in both RAS groups in the cortex and medulla (Figure 1e,g,h), but MetS-RAS elicited great loss in the cortex compared with RAS (Figure 1e,g).

Perirenal angiogenic activity

In stained slides, RAS increased VEGF expression in the renal artery wall in both the endothelium and adventitia (Figure 2a), but not in perirenal fat (Figure 2b). Contrarily, MetS decreased VEGF in the renal artery wall and kidney tissue (Figure 2c) in RAS but upregulated it in the perirenal

Table 1. Characteristics of normal and RAS pigs with or without MetS ($n = 7$ each)

	Normal	RAS	MetS-RAS
Body weight (kg)	52.3 ± 0.7	50.2 ± 2.5	92.4 ± 2.3*
Degree of stenosis (%)	–	64.8 ± 3.8	65.0 ± 5.0
MAP (mm Hg)	89.6 ± 2.1	97.2 ± 2.0*	129.6 ± 9.1*†
Creatinine (mg/dl)	1.2 ± 0.1	1.6 ± 0.1*	1.7 ± 0.1*
Total cholesterol (mg/dl)	71 (67.5–84)	91 (79.2–106.5)	506 (365.2–723.2)*†
Triglyceride (mg/dl)	7.0 ± 0.3	11.9 ± 0.9	15.1 ± 3.0*
LDL cholesterol (mg/dl)	26.6 (22–31.7)	39.2 (34–44.4)	444 (277.4–555.2)*†
Urine ACR (mg/g)	9.9 (4.4–20.6)	16.2 (13.3–536.4)	12.0 (5.4–79.9)

Data are mean ± SEM or median (interquartile range). Abbreviations: ACR, albumin to creatinine ratio; LDL, low-density lipoprotein; MAP, mean arterial pressure; MetS, metabolic syndrome; RAS, renal artery stenosis.

*$P < 0.05$ vs. normal.

†$P < 0.05$ vs. RAS.

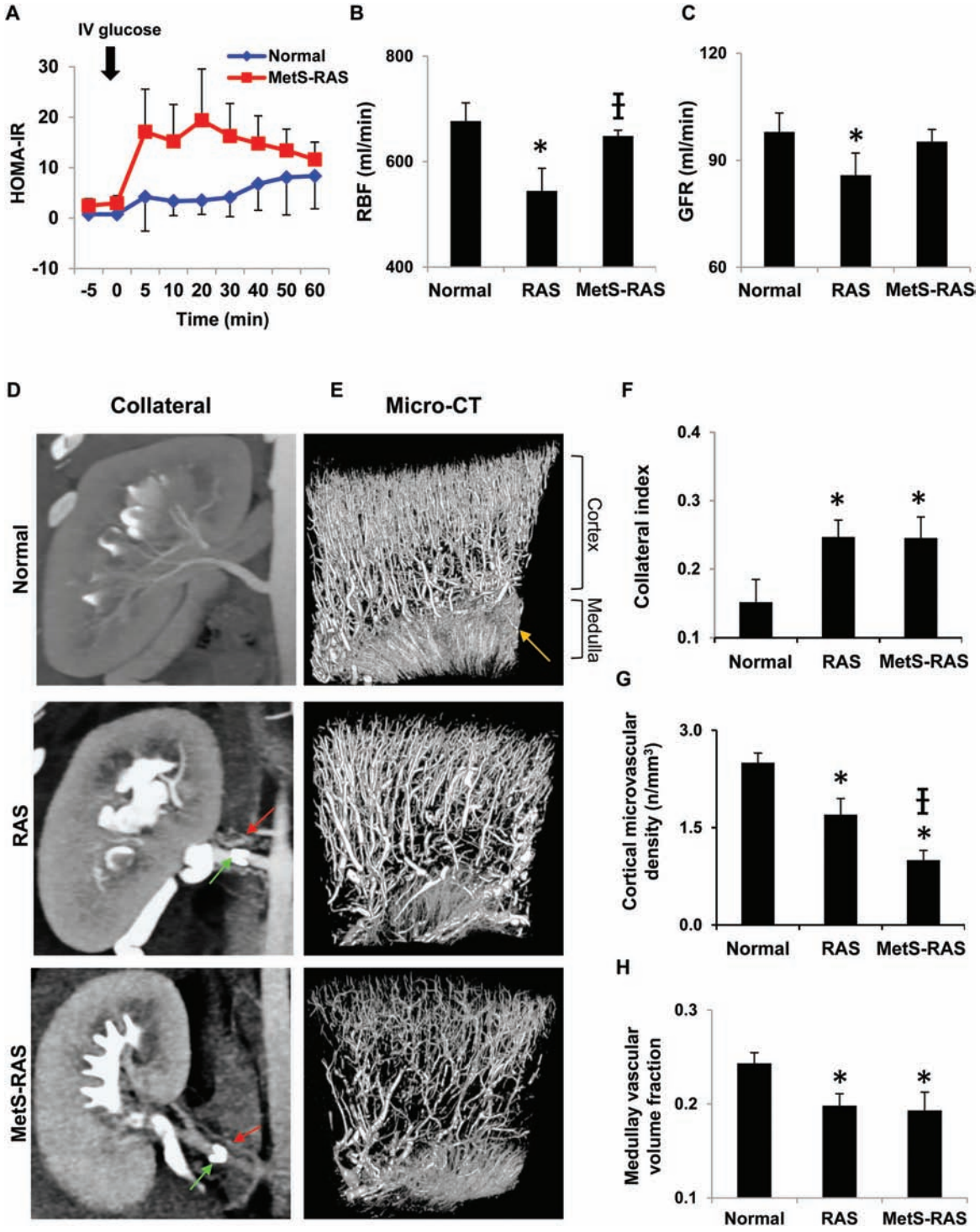

Figure 1. Establishment of MetS in domestic pigs with RAS and changes in renal function and circulation compared to Normal and RAS alone. Intravenous glucose tolerance test showing increased HOMA-IR index in animals with the MetS-RAS compared with normal animals, suggesting insulin resistance (**a**). RBF and GFR significantly decreased in pigs with RAS, but not when RAS was accompanied by MetS (**b**, **c**). Representative multidetector- and micro-CT images showing collateral circulation (**d**), intrarenal cortical microvascular density and medullary vascular volume fraction (**e**), and their quantification (**g, h**). Collateral index was similarly elevated in RAS and MetS-RAS, but MetS-RAS had greater cortical microvascular loss (**f**). *$P < 0.05$ vs. normal, †$P < 0.05$ vs. RAS. Green arrow: coil inducing stenosis; red arrow: collateral vessels; orange arrow: vasa recta in medulla. (Please refer to color online only for indicated colors.) Abbreviations: CT, computed tomography; GFR, glomerular filtration rate; HOMA-IR, homeostasis model assessment of insulin resistance; MetS, metabolic syndrome; MetS-RAS, metabolic syndrome and renal artery stenosis; RAS, renal artery stenosis; RBF, renal blood flow.

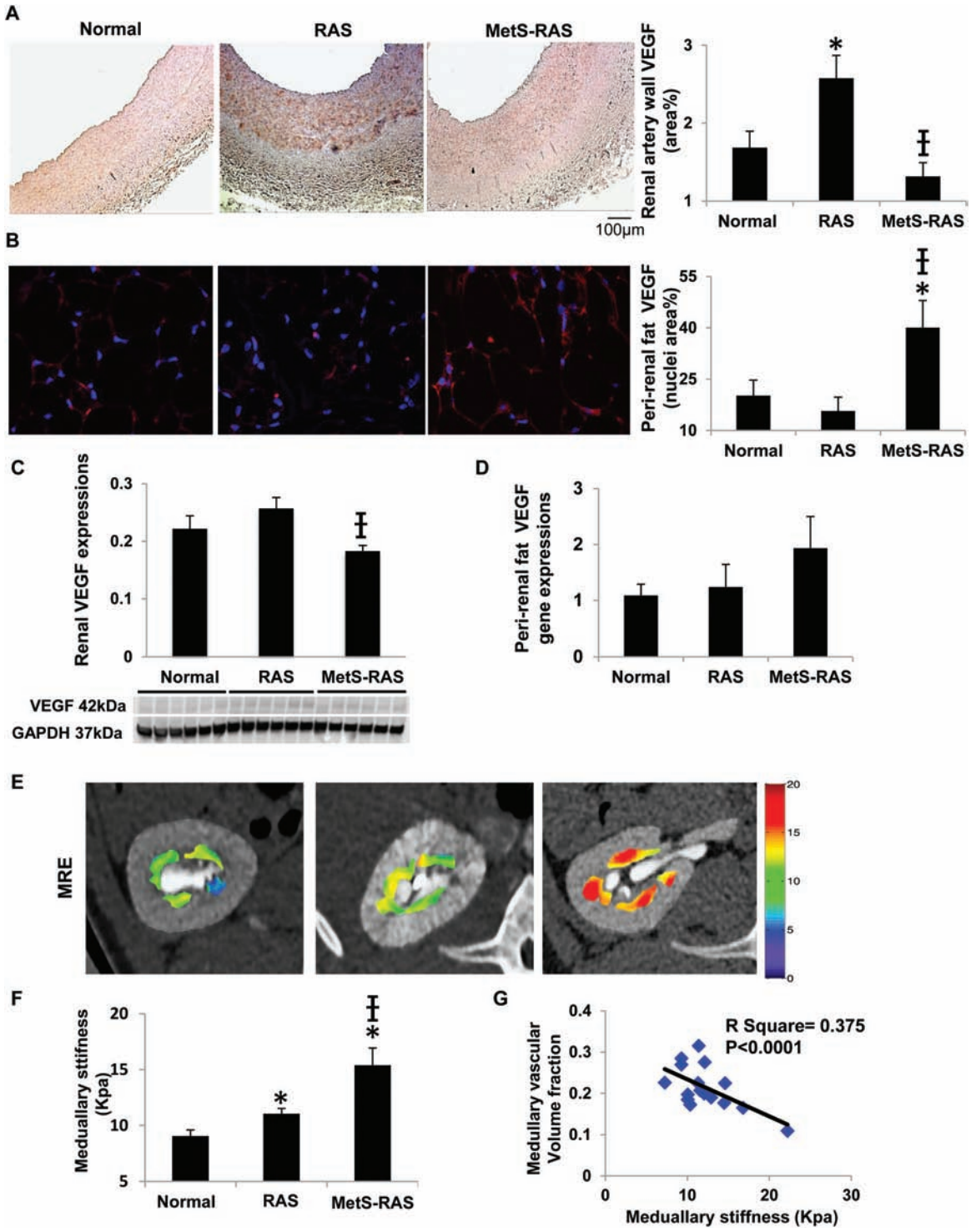

Figure 2. Expression of angiogenic VEGF in renal artery wall and fat tissue, and association of medullary vascular volume fraction with stiffness. Expression of VEGF in the renal artery wall (**a**) and perirenal fat (**b**, red). RAS increased VEGF expression in the renal artery wall, whereas MetS-RAS decreased VEGF in the renal artery wall but increased it in the perirenal fat. Renal protein expression of VEGF was decreased in MetS-RAS compared with RAS (**c**). VEGF gene expression in perirenal fat was not different among the groups (**d**). Renal medullary stiffness by MRE (yellow/red indicates greater stiffness) and its quantification (**e**, **f**). (Please refer to color online-only for indicated colors.) An inverse correlation was observed between medullary stiffness and vascular volume fraction (**g**). *$P < 0.05$ vs. normal, †$P < 0.05$ vs. RAS. Abbreviations: MetS-RAS, metabolic syndrome and renal artery stenosis; MRE, magnetic resonance elastography; RAS, renal artery stenosis; VEGF, vascular endothelial growth factor.

fat. VEGF gene expression in perirenal fat of MetS-RAS showed a similar pattern, although this has not reached statistical significance levels (Figure 2d).

Renal fibrosis and stiffness

An increase in the stenotic kidney medullary stiffness *in vivo* was found in RAS, was greater in MetS-RAS (Figure 2e,f), and was inversely correlated with vascular volume fraction (Figure 2g). Trichrome staining *ex vivo* showed increased cortical and medullary fibrosis in both RAS groups, which was markedly greater in MetS-RAS (Figure 3a–c). Glomerulosclerosis was similarly increased in both RAS groups compared with normal (Figure 3d).

Renal tubular injury, inflammation, and EndoMT

Tubular injury scores evaluated in periodic acid–Schiff staining increased in stenotic compared with normal kidneys and further in MetS-RAS compared with RAS (Figure 3b,e). Expressions of monocyte chemoattractant protein-1 and TNF-α were significantly higher in MetS-RAS than normal and RAS (Figure 4a–d). CD31 and Vimentin colocalization was greater in MetS-RAS than in RAS as well as normal kidneys, suggesting increased EndoMT (Figure 4e,f).

DISCUSSION

In the present study, we found that while swine MetS-RAS kidneys maintained normal RBF and GFR, they did not magnify development of collateral circulation compared with RAS. This observation suggests that collateral growth is unlikely to be a major contributor to preserved renal hemodynamics and function in MetS-RAS. Furthermore, in spite of renal hemodynamics within the normal range, MetS-RAS aggravated renal injury distal to the stenosis, including loss of cortical microvasculature and increased fibrosis, tubular injury, inflammation, and stiffness compared with RAS, suggesting that at an early stage, preserved renal function in MetS may be partly dissociated from the downstream parenchymal damage.

Establishment of collateral circulation is thought to play important roles in maintaining renal blood supply when the renal artery is obstructed.[8,30] Earlier studies have found that collateral development is influenced by the degree of obstruction and by availability of extrarenal arterial sources that carry the collateral flow.[30] Importantly, the underlying condition of the kidney might be an important determinant of both the degree and effectiveness of the newly established circulation to sustain renal blood supply.[30]

In our swine model, development of collateral circulation in MetS-RAS was similar to that observed in RAS alone and could be affected by multifactorial mechanisms. Obesity and MetS activate proangiogenic pathways, possibly mediated through inflammatory mechanisms that stimulate intrarenal angiogenesis[11,31] and might hypothetically also augment collateral vessel formation. Notably, MetS-RAS increased VEGF expression in perirenal fat, as observed by others.[32] This might be related to the adipose-enriched inhibitor of DNA binding protein-3, which promotes VEGF expression and microvascular blood volume in visceral fat.[32]

On the other hand, when coexisting with RAS, MetS may synergize with injury mechanisms activated in the poststenotic kidney to magnify microvascular loss by amplifying increases in oxidative stress characteristic of both RAS and MetS.[11] In addition, increased fibrogenic activity in the poststenotic kidney[33,34] can also suppress angiogenic signaling and inhibit angiogenesis and arteriogenesis.[35] Indeed, MetS-RAS pigs were inclined to have greater renal fibrosis both *in vivo* and *ex vivo*, as well as intrarenal microvascular rarefaction. Factors including insulin resistance and dyslipidemia may induce endothelial dysfunction and EndoMT,[36] which might in turn contribute to development and progression of renal fibrosis in MetS-RAS. Hence, the distinct patterns of intrarenal injury in MetS-RAS may partly compromise the capability of the stenotic kidney to sustain its microcirculation. Furthermore, insulin resistance has been shown to impair the function of angiogenic progenitor cells that participate in endothelial repair and thereby delay endothelial regeneration.[37] This may not only jeopardize within the MetS kidney microvascular repair, facilitating microvascular regression compared with RAS alone, but may also lessen the response of endothelial cells in renal artery and surrounding vessels to the ischemic stimulus for angiogenesis.

We have also found increased inflammation in MetS-RAS compared with RAS kidneys, indicated by upregulation of MCP-1 and TNF-α, implicating inflammation in the amplified kidney injury in MetS-RAS. In addition, greater inflammation and oxidative stress in perirenal fat cause endothelial dysfunction of the adjacent renal arteries, partly due to paracrine TNF-α signaling.[38] Blunted upregulation of VEGF expression in MetS-RAS renal artery wall compared with RAS might have been related to the poststenotic kidney, as well as local arterial or perirenal fat *milieu*. Collectively, their net result was collateral vessels channeling similar to that in RAS.[4] Hence, regardless of the mechanisms involved, given its preserved RBF and GFR in the face of a similar collateral index to RAS, our study argues against collateral circulation growth as a chief determinant of sustained function in the poststenotic kidney coexisting with MetS.

Although the stenotic kidney function was comparable with normal pigs, elevated plasma creatinine indicated decline of overall renal function in MetS-RAS, suggesting impaired contralateral kidney function, possibly due to greater hypertension or to cytokines released from the obese stenotic kidney.[39] Contrarily, renal protein excretion was unaffected, due to the early stage and modest glomerular injury. Whether the contralateral kidney influences the growth of collateral vessels should be further examined.

Limitations

Our study is limited by short duration of the disease, yet renal physiology and pathophysiology in our model resemble those in humans, and thus, our study has translational power. We cannot rule out the possibility that collateral vessels smaller than the resolution of our CT scanner were overlooked (<0.02 mm). However, many native collateral vessels

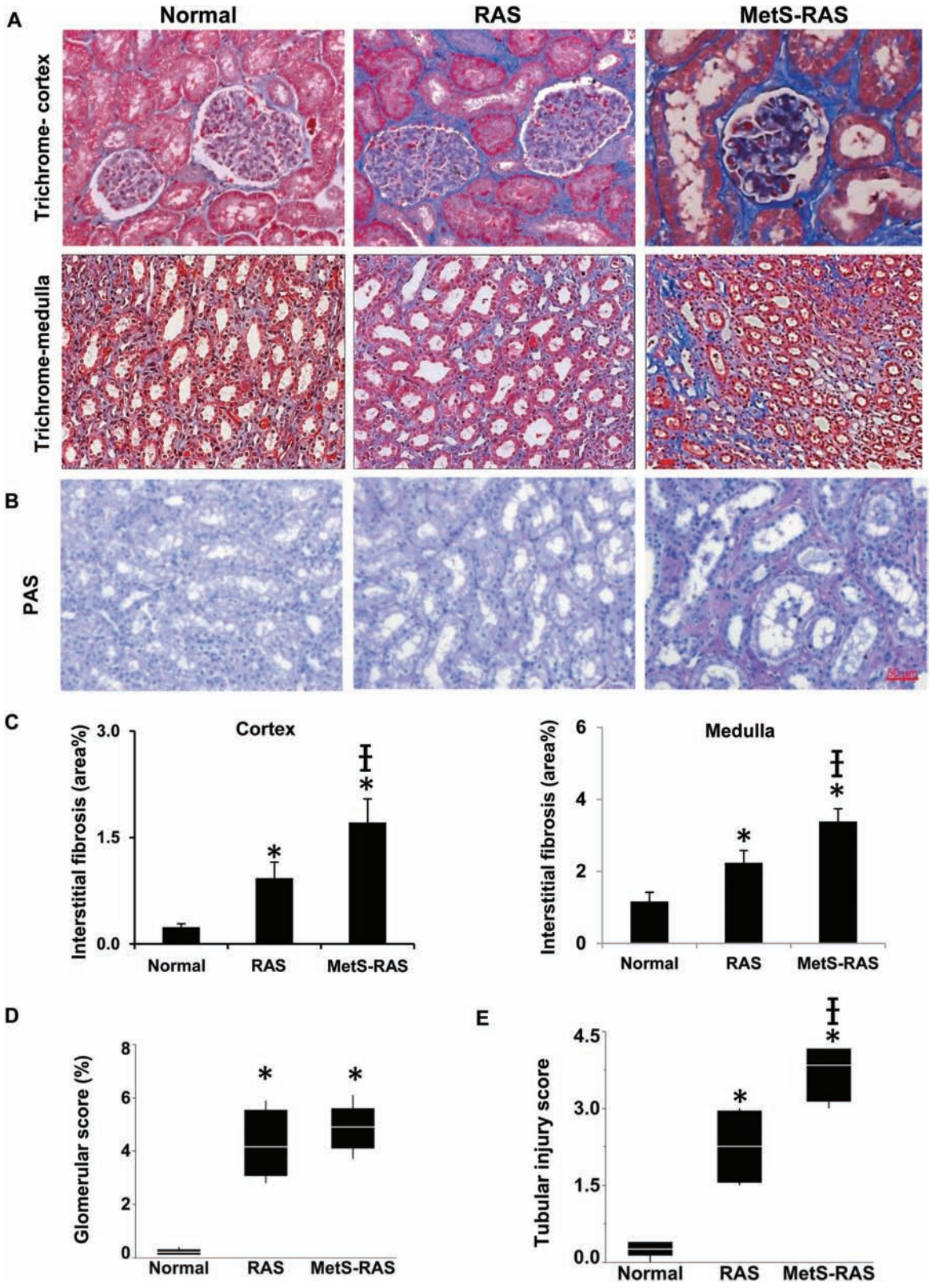

Figure 3. Kidney tissue injury in RAS and MetS-RAS pigs. Interstitial fibrosis and glomerulosclerosis in the stenotic kidney increased in RAS and MetS-RAS compared with normal (**a**, **c**, **d**). MetS-RAS induced greater tissue scarring in both cortex and medulla. Tubular injury scores evaluated in PAS staining were increased in the stenotic kidney compared with normal kidney and in MetS-RAS vs. RAS (**b**, **e**). *$P < 0.05$ vs. normal, †$P < 0.05$ vs. RAS. Abbreviations: MetS-RAS, metabolic syndrome and renal artery stenosis; PAS, periodic acid–Schiff; RAS, renal artery stenosis.

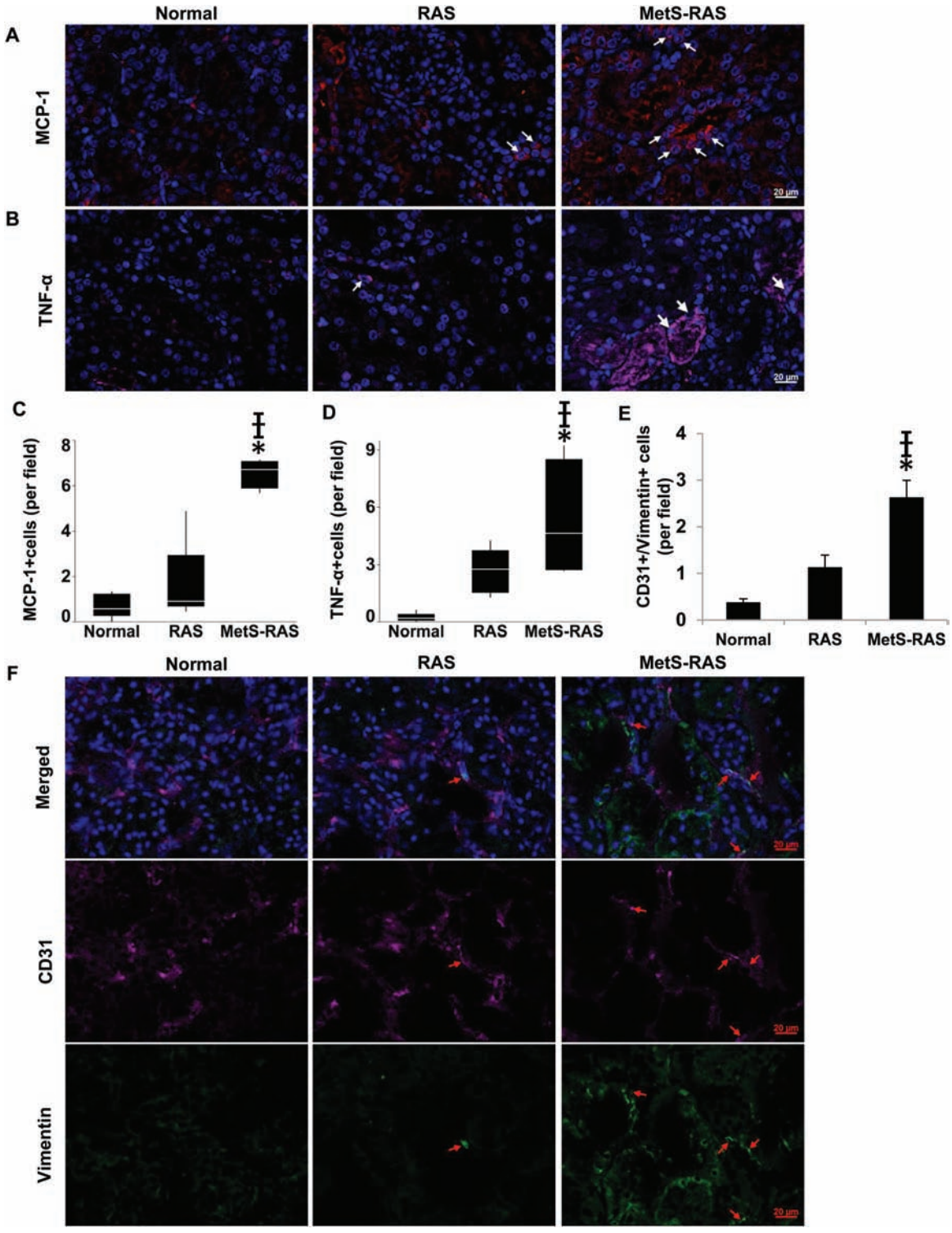

Figure 4. In immunofluorescence, MCP-1-expressing cells (red) were more abundant in MetS-RAS compared with normal and RAS (**a**, **c**), as was TNF-α expression (pink) (**b**, **d**). CD31 (pink) and Vimentin (green) colocalization was higher in MetS-RAS than in RAS and normal, suggesting increased endothelial to mesenchymal transition (**e**, **f**). (Please refer to color online only for indicated colors). *$P < 0.05$ vs. normal, †$P < 0.05$ vs. RAS. Abbreviations: MCP-1, monocyte chemoattractant protein-1; MetS-RAS, metabolic syndrome and renal artery stenosis; RAS, renal artery stenosis; TNF-α, tumor necrosis factor-alpha.

are considered to be visible angiographically.[30] Medullary vascular volume fraction in MetS-RAS exhibited larger variability than cortical microvascular density, possibly due to relatively smaller medullary size compared with cortex. The mechanisms underlying the development, progression, and patterns of the collateral vessels (e.g., their origin and

termination) in normal and MetS kidneys need to be pursued in future studies. The mechanisms that sustain measurable renal function in the presence of amplified tissue injury in MetS-RAS also warrant additional studies.

In conclusion, this study shows that the kidney distal to RAS coexisting with obesity metabolic disorders had relatively preserved hemodynamics, despite collateral circulation growth being comparable with that observed in RAS alone. These findings suggest that the collateral circulation is unlikely a major contributor to blood flow maintenance in MetS-RAS; its complex mechanisms should be further investigated.

ACKNOWLEDGMENTS

This study was partly supported by National Institute of Health (NIH) grant numbers DK102325, DK104273, HL123160, and C06-RR018898.

DISCLOSURE

The authors declared no conflict of interest.

REFERENCES

1. Colyer WR Jr, Cooper CJ. Cardiovascular morbidity and mortality and renal artery stenosis. *Prog Cardiovasc Dis* 2009; 52:238–242.
2. Weber BR, Dieter RS. Renal artery stenosis: epidemiology and treatment. *Int J Nephrol Renovasc Dis* 2014; 7:169–181.
3. Burlacu A, Siriopol D, Voroneanu L, Nistor I, Hogas S, Nicolae A, Nedelciuc I, Tinica G, Covic A. Atherosclerotic renal artery stenosis prevalence and correlations in acute myocardial infarction patients undergoing primary percutaneous coronary interventions: data from nonrandomized single-center study (REN-ACS)—a single center, prospective, observational study. *J Am Heart Assoc* 2015; 4:e002379.
4. Abrams HL, Cornell SH. Patterns of collateral flow in renal ischemia. *Radiology* 1965; 84:1001–1012.
5. Brolin I, Stener I. Collaterals in obstruction of the renal artery. *Acta Radiol Diagn (Stockh)* 1966; 4:449–462.
6. Boijsen E. Angiographic studies of the anatomy of single and multiple renal arteries. *Acta Radiol Suppl* 1959; 183:1–135.
7. Itzchak Y, Deutsch V, Adar R, Mozes M. Angiography of renal capsular complex in normal and pathological conditions and its diagnostic implications. *CRC Crit Rev Clin Radiol Nucl Med* 1974; 5:111–144.
8. Hietala SO, Kunz R. Collateral circulation in stenosis or occlusion of the renal artery. *Cardiovasc Radiol* 1979; 2:249–255.
9. Krier JD, Crane JA, Eirin A, Zhu XY, Lerman A, Lerman LO. Hemodynamic determinants of perivascular collateral development in swine renal artery stenosis. *Am J Hypertens* 2013; 26:209–217.
10. Perlstein TS, Gerhard-Herman M, Hollenberg NK, Williams GH, Thomas A. Insulin induces renal vasodilation, increases plasma renin activity, and sensitizes the renal vasculature to angiotensin receptor blockade in healthy subjects. *J Am Soc Nephrol* 2007; 18:944–951.
11. Zhang X, Li ZL, Woollard JR, Eirin A, Ebrahimi B, Crane JA, Zhu XY, Pawar AS, Krier JD, Jordan KL, Tang H, Textor SC, Lerman A, Lerman LO. Obesity-metabolic derangement preserves hemodynamics but promotes intrarenal adiposity and macrophage infiltration in swine renovascular disease. *Am J Physiol Renal Physiol* 2013; 305:F265–F276.
12. Pawar AS, Zhu XY, Eirin A, Tang H, Jordan KL, Woollard JR, Lerman A, Lerman LO. Adipose tissue remodeling in a novel domestic porcine model of diet-induced obesity. *Obesity (Silver Spring)* 2015; 23:399–407.
13. Li Z, Woollard JR, Wang S, Korsmo MJ, Ebrahimi B, Grande JP, Textor SC, Lerman A, Lerman LO. Increased glomerular filtration rate in early metabolic syndrome is associated with renal adiposity and microvascular proliferation. *Am J Physiol Renal Physiol* 2011; 301:F1078–F1087.
14. Lerman LO, Schwartz RS, Grande JP, Sheedy PF, Romero JC. Noninvasive evaluation of a novel swine model of renal artery stenosis. *J Am Soc Nephrol* 1999; 10:1455–1465.
15. Lerman LO, Nath KA, Rodriguez-Porcel M, Krier JD, Schwartz RS, Napoli C, Romero JC. Increased oxidative stress in experimental renovascular hypertension. *Hypertension* 2001; 37:541–546.
16. Chade AR, Rodriguez-Porcel M, Grande JP, Krier JD, Lerman A, Romero JC, Napoli C, Lerman LO. Distinct renal injury in early atherosclerosis and renovascular disease. *Circulation* 2002; 106:1165–1171.
17. Zhang X, Eirin A, Li ZL, Crane JA, Krier JD, Ebrahimi B, Pawar AS, Zhu XY, Tang H, Jordan KL, Lerman A, Textor SC, Lerman LO. Angiotensin receptor blockade has protective effects on the poststenotic porcine kidney. *Kidney Int* 2013; 84:767–775.
18. Daghini E, Primak AN, Chade AR, Krier JD, Zhu XY, Ritman EL, McCollough CH, Lerman LO. Assessment of renal hemodynamics and function in pigs with 64-section multidetector CT: comparison with electron-beam CT. *Radiology* 2007; 243:405–412.
19. Warner L, Yin M, Glaser KJ, Woollard JA, Carrascal CA, Korsmo MJ, Crane JA, Ehman RL, Lerman LO. Noninvasive in vivo assessment of renal tissue elasticity during graded renal ischemia using MR elastography. *Invest Radiol* 2011; 46:509–514.
20. Korsmo MJ, Ebrahimi B, Eirin A, Woollard JR, Krier JD, Crane JA, Warner L, Glaser K, Grimm R, Ehman RL, Lerman LO. Magnetic resonance elastography noninvasively detects in vivo renal medullary fibrosis secondary to swine renal artery stenosis. *Invest Radiol* 2013; 48:61–68.
21. Ebrahimi B, Gloviczki M, Woollard JR, Crane JA, Textor SC, Lerman LO. Compartmental analysis of renal BOLD MRI data: introduction and validation. *Invest Radiol* 2012; 47:175–182.
22. Zhu XY, Chade AR, Rodriguez-Porcel M, Bentley MD, Ritman EL, Lerman A, Lerman LO. Cortical microvascular remodeling in the stenotic kidney: role of increased oxidative stress. *Arterioscler Thromb Vasc Biol* 2004; 24:1854–1859.
23. Zhu XY, Rodriguez-Porcel M, Bentley MD, Chade AR, Sica V, Napoli C, Caplice N, Ritman EL, Lerman A, Lerman LO. Antioxidant intervention attenuates myocardial neovascularization in hypercholesterolemia. *Circulation* 2004; 109:2109–2115.
24. Ebrahimi B, Li Z, Eirin A, Zhu XY, Textor SC, Lerman LO. Addition of endothelial progenitor cells to renal revascularization restores medullary tubular oxygen consumption in swine renal artery stenosis. *Am J Physiol Renal Physiol* 2012; 302:F1478–F1485.
25. Livak KJ, Schmittgen TD. Analysis of relative gene expression data using real-time quantitative PCR and the 2(-Delta Delta C(T)) Method. *Methods* 2001; 25:402–408.
26. Eirin A, Zhu XY, Puranik AS, Tang H, McGurren KA, van Wijnen AJ, Lerman A, Lerman LO. Mesenchymal stem cell-derived extracellular vesicles attenuate kidney inflammation. *Kidney Int* 2017; 92:114–124.
27. Zhang X, Krier JD, Amador Carrascal C, Greenleaf JF, Ebrahimi B, Hedayat AF, Textor SC, Lerman A, Lerman LO. Low-energy shockwave therapy improves ischemic kidney microcirculation. *J Am Soc Nephrol* 2016; 27:3715–3724.
28. Eirin A, Zhu XY, Ebrahimi B, Krier JD, Riester SM, van Wijnen AJ, Lerman A, Lerman LO. Intrarenal delivery of mesenchymal stem cells and endothelial progenitor cells attenuates hypertensive cardiomyopathy in experimental renovascular hypertension. *Cell Transplant* 2015; 24:2041–2053.
29. Song S, Zhang M, Yi Z, Zhang H, Shen T, Yu X, Zhang C, Zheng X, Yu L, Ma C, Liu Y, Zhu D. The role of PDGF-B/TGF-β1/neprilysin network in regulating endothelial-to-mesenchymal transition in pulmonary artery remodeling. *Cell Signal* 2016; 28:1489–1501.
30. Yune HY, Klatte EC. Collateral circulation to an ischemic kidney. *Radiology* 1976; 119:539–546.
31. Li ZL, Woollard JR, Ebrahimi B, Crane JA, Jordan KL, Lerman A, Wang SM, Lerman LO. Transition from obesity to metabolic syndrome is associated with altered myocardial autophagy and apoptosis. *Arterioscler Thromb Vasc Biol* 2012; 32:1132–1141.
32. Cutchins A, Harmon DB, Kirby JL, Doran AC, Oldham SN, Skaflen M, Klibanov AL, Meller N, Keller SR, Garmey J, McNamara CA. Inhibitor of differentiation-3 mediates high fat diet-induced visceral fat expansion. *Arterioscler Thromb Vasc Biol* 2012; 32:317–324.
33. Chade AR, Rodriguez-Porcel M, Grande JP, Zhu X, Sica V, Napoli C, Sawamura T, Textor SC, Lerman A, Lerman LO. Mechanisms of renal

structural alterations in combined hypercholesterolemia and renal artery stenosis. *Arterioscler Thromb Vasc Biol* 2003; 23:1295–1301.
34. Gloviczki ML, Keddis MT, Garovic VD, Friedman H, Herrmann S, McKusick MA, Misra S, Grande JP, Lerman LO, Textor SC. TGF expression and macrophage accumulation in atherosclerotic renal artery stenosis. *Clin J Am Soc Nephrol* 2013; 8:546–553.
35. Geng L, Chaudhuri A, Talmon G, Wisecarver JL, Wang J. TGF-Beta suppresses VEGFA-mediated angiogenesis in colon cancer metastasis. *PLoS One* 2013; 8:e59918.
36. Souilhol C, Harmsen MC, Evans PC, Krenning G. Endothelial-mesenchymal transition in atherosclerosis. *Cardiovasc Res* 2018; 114:565–577.
37. Kahn MB, Yuldasheva NY, Cubbon RM, Smith J, Rashid ST, Viswambharan H, Imrie H, Abbas A, Rajwani A, Aziz A, Baliga V, Sukumar P, Gage M, Kearney MT, Wheatcroft SB. Insulin resistance impairs circulating angiogenic progenitor cell function and delays endothelial regeneration. *Diabetes* 2011; 60:1295–1303.
38. Ma S, Zhu XY, Eirin A, Woollard JR, Jordan KL, Tang H, Lerman A, Lerman LO. Perirenal fat promotes renal arterial endothelial dysfunction in obese swine through tumor necrosis factor-α. *J Urol* 2016; 195:1152–1159.
39. Eirin A, Gloviczki ML, Tang H, Gössl M, Jordan KL, Woollard JR, Lerman A, Grande JP, Textor SC, Lerman LO. Inflammatory and injury signals released from the post-stenotic human kidney. *Eur Heart J* 2013; 34:540–548a.